OPEN ACCESS Freely available online

PLOS ONE

Non-Equilibrium Casimir Force between Vibrating Plates

Andreas Hanke*

Department of Physics, University of Texas at Brownsville, Brownsville, Texas, United States of America

Abstract

We study the fluctuation-induced, time-dependent force between two plates confining a correlated fluid which is driven out of equilibrium mechanically by harmonic vibrations of one of the plates. For a purely relaxational dynamics of the fluid we calculate the fluctuation-induced force generated by the vibrating plate on the plate at rest. The time-dependence of this force is characterized by a positive lag time with respect to the driving. We obtain two distinctive contributions to the force, one generated by diffusion of stress in the fluid and another related to resonant dissipation in the cavity. The relation to the dynamic Casimir effect of the electromagnetic field and possible experiments to measure the time-dependent Casimir force are discussed.

Citation: Hanke A (2013) Non-Equilibrium Casimir Force between Vibrating Plates. PLoS ONE 8(1): e53228. doi:10.1371/journal.pone.0053228

Editor: Jörg Langowski, German Cancer Research Center, Germany

Received November 19, 2011; **Accepted** November 29, 2012; **Published** January 10, 2013

Funding: This work was supported by the Air Force Office of Scientific Research under Grant No. FA9550-10-1-0408. The funders had no role in study design, data collection and analysis, decision to publish, or preparation of the manuscript.

Competing Interests: The author has declared that no competing interests exist.

* E-mail: hanke@phys.utb.edu

Introduction

A fundamental advance in the understanding of nature was the insight that physical forces between bodies, instead of operating at a distance, are generated by *fields*; the latter obeying their own dynamics, implying a finite speed of propagation of signals and causality [1]. Moreover, time-varying fields can sustain themselves in otherwise empty space to produce disembodied waves; exemplified by electromagnetic fields and waves, and gravitational fields. Gravitational waves are believed to be detected in the near future [2].

Another force seemingly operating at a distance is the Casimir force. This force was first predicted by Casimir in 1948 for two parallel conducting plates in vacuum, separated by a distance L, for which he found an attractive force per unit area $F/A = -\pi^2\hbar c/(240L^4)$ [3]. It can be understood as resulting from the modification of quantum-mechanical zero-point fluctuations of the electromagnetic field due to confining boundaries [4–7]. In the last decade, high-precision measurements of the Casimir force have become available which confirm Casimir's prediction within a few per cent [8–11]; recent experiments demonstrate the possibility of using the Casimir force as an actuation force for movable elements in nanomechanical systems [10–12]. The thermal Casimir force, generated by thermal rather than quantum fluctuations of the electromagnetic field, has recently been confirmed [13]. This development goes along with significant advances in calculating the Casimir force for complex geometries and materials [7,14–21]. A force analogous to the electromagnetic Casimir force occurs if the fluctuations of the confined medium are of thermal instead of quantum origin [5,22,23]. The thermal analog of the Casimir effect, referred to as critical Casimir effect, was first predicted by Fisher and de Gennes for the concentration fluctuations of a binary liquid mixture close to its critical demixing point confined by boundaries [24]; recently, the critical Casimir effect was quantitatively confirmed for this very system [25]. (For computational methods concerning the calculation of critical Casimir forces, see, e.g., Refs. [26–28].)

The vast majority of work done on the Casimir effect, and fluctuation-induced forces in general, pertain to the equilibrium case. That is, the system is in its quantal ground state in case of the electromagnetic Casimir effect, or in thermodynamic equilibrium in case of the thermal analog. A number of recent experiments probe the Casimir force between moving components in nanomechanical systems [10–12], and effects generated by moving boundaries have been studied, e.g., for Casimir force driven ratchets [29]; however, the data are usually compared with predictions for the Casimir force obtained for systems at rest, corresponding to a quasi-static approximation.

Distinct new effects occur if the fluctuating medium is driven out of equilibrium. In this case the observed effects become sensitive to the dynamics governing the fluctuating medium, which may lead to a better understanding of these systems and may provide new control parameters to manipulate them [30–40]. The generalization of the electromagnetic Casimir effect to systems with moving boundaries, referred to as dynamic Casimir effect, exhibits friction of moving mirrors in vacuum and the creation of photons [41–44]. Related effects due to oscillating media [45], and nonequilibrium Casimir-Polder forces on moving atoms [46], have also been considered. Interesting effects occur if each body immersed in the fluctuating electromagnetic field is at a different temperature [47,48]. The associated nonequilibrium Casimir forces and heat transfer between the bodies lead to observable effects [49,50]. For the thermal analog, fluctuation-induced forces in non-equilibrium systems have been studied in the context of the Soret effect, which occurs in the presence of an external temperature gradient [31]. Effects of temperature changes in classical free scalar field theories and thermal drag forces have been studied in [32–35]; however, recently it was argued that the method presented in [32–35] is invalid to obtain the fluctuation-induced force exerted on an inclusion or plate embedded in the medium, whereas the stress tensor method, as used in the present

work, yields the correct force [40]. Fluctuation-induced forces have also been obtained for macroscopic bodies immersed in mechanically driven systems [30], granular fluids [36], and reaction-diffusion systems [37]. Recently it was shown that non-equilibrium fluctuations can induce self-forces on single, asymmetric objects, and may lead to a violation of the action-reaction principle between two objects [38].

In this work we consider a correlated fluid driven out of equilibrium mechanically by a vibrating plate, and study the resulting fluctuation-induced, time-dependent force $F(t)$ on a second plate at rest. We wish to study the time-dependence of this force in view of the finite speed of diffusion of perturbations in the fluctuating medium, and causality. We consider the simplest possible dynamics of the medium between the plates, namely the purely relaxational dynamics of model A. Specifically, we consider two infinitely extended plates parallel to the xy-plane, where plate 1 is at rest while plate 2 is vibrating parallel to the z-direction by some external driving, resulting in a time-dependent separation (see Fig. 1)

$$L(t) = L_0 + a\cos(\omega_0 t) \tag{1}$$

with amplitude a and driving frequency ω_0. The fluctuating medium is described by a non-conserved scalar order parameter field $\phi(\mathbf{r},t)$, corresponding to the critical dynamics of model A [51,52], subject to Dirichlet boundary conditions $\phi = 0$ at the plates. The field ϕ may describe the order parameter of a fluid thermodynamically close to a critical point, or a massless Goldstone mode arising from the breaking of a continuous symmetry such as in nematic liquid crystals or superfluid ^{4}He [5,22]. Our results hold in Gaussian approximation right at the critical point T_c for which the bulk correlation length ξ diverges. For $T \neq T_c$ the fluctuation-induced force also depends on the finite correlation length ξ. Moreover, for near-critical fluids and binary liquid mixtures the boundary conditions at confining walls correspond to the so-called normal rather than Dirichlet surface universality class [22]. However, it should be noted that dynamic critical behavior is less universal than equilibrium critical behavior. For example, for the liquid-gas transition and the demixing transition in a binary liquid mixture a conserved order parameter convects with the conserved transverse momentum current of the fluid, resulting in critical dynamics referred to as model H [53]; conversely, the superfluid transition of ^{4}He corresponds to critical dynamics of model F [54]. In addition, critical dynamics of real fluids may be modified by effects due to gravity and the coupling of the order parameter to secondary densities, which further complicates a quantitative comparison of theory and experiment (see [51,52] for reviews). Strictly speaking, purely relaxational dynamics of a non-conserved scalar order parameter corresponding to model A only applies to uniaxial magnetic systems and simple lattice gases. However, the results and conclusions derived here for model A dynamics yield new insight in non-equilibrium behavior and may serve as a starting point for more realistic models.

Our results for the time-dependent force $F(t)$ on plate 1 hold to first order in a (cf. Eq. (1)). As shown in Fig. 1, $F(t)$ is the sum of forces $F_+(t)$ and F_- acting on opposite sides of the plate; $F_+(t)$ being the force acting on plate 1 from the side of the cavity, and F_- the (time-independent) force on the boundary surface of a semi-infinite half-space filled with the fluctuating medium. The net force $F(t) = F_+(t) + F_-$ is expected to be finite and overall attractive, i.e., directed towards plate 2.

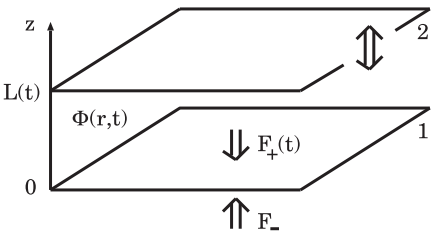

Figure 1. Geometry of two parallel plates separated by a varying distance $L(t)$. Plate 1 is at rest while plate 2 is vibrating parallel to the z-direction. The plates are immersed in a fluctuating medium with purely relaxational dynamics described by a non-conserved scalar order parameter $\phi(\mathbf{r},t)$. The fluctuation-induced, time-dependent net force $F(t)$ on plate 1 is the sum of forces $F_+(t)$ and F_- acting on opposite sides of the plate.
doi:10.1371/journal.pone.0053228.g001

Results

Relaxational Dynamics

In traditional studies of the fluctuation-induced force between two plates, both plates are assumed to be at rest at constant separation L_0 (see Fig. 1). The system is in thermal equilibrium and the fluctuations of the order parameter ϕ are described by the statistical Boltzmann weight $e^{-\beta H}$ with Gaussian Hamiltonian

$$\beta H\{\phi\} = \frac{1}{2}\int d^3r(\nabla\phi)^2, \tag{2}$$

where $\beta = 1/(k_B T)$ with the Boltzmann constant k_B and the temperature T (assumed to be constant). The fluctuation-induced force F_0 on plate 1 per unit area A is found to be [5,22,23]

$$\frac{F_0}{A} = -\frac{\zeta(3)}{8\pi}\frac{k_B T}{L_0^3}, \tag{3}$$

where the minus sign indicates that the force is attractive. Equation (3) is a universal result, independent of the underlying dynamics of the fluctuating medium, as long as the equilibrium is described by Eq. (2).

We now turn to the case where plate 2 is vibrating parallel to the z-direction, resulting in a time-dependent separation $L(t)$ between the plates (see Eq. (1) and Fig. 1). The time-dependent boundary conditions for the order parameter $\phi(\mathbf{r},t)$ in the medium between the plates now drive the system out of equilibrium. Locally, the order parameter will relax back to equilibrium according to the dynamics of the medium; in this work, we consider a purely relaxational dynamics described by the Langevin equation (see, e.g., Chapter 8 in Ref. [55], and references cited therein)

$$\gamma\frac{\partial}{\partial t}\phi(\mathbf{r},t) = \nabla^2\phi(\mathbf{r},t) + \eta(\mathbf{r},t) \tag{4}$$

where γ is the friction coefficient. The random force $\eta(\mathbf{r},t)$ is assumed to have zero mean and to obey the fluctuation-dissipation relation

$$\langle\eta(\mathbf{r},t)\eta(\mathbf{r}',t')\rangle = 2\gamma k_B T\delta^{(3)}(\mathbf{r}-\mathbf{r}')\delta(t-t') \tag{5}$$

where the brackets $\langle\ \rangle$ denote a local, stochastic average and $\delta^{(3)}$ is the delta function in 3 dimensions.

Non-Equilibrium Casimir Force

The force per unit area acting on plate 1 from the side of the cavity can be expressed as $F_+(t)/A=\lim_{z\to 0}\langle T_{zz}(\mathbf{r}_\parallel,z,t)\rangle$ where $\mathbf{r}_\parallel=(x,y)$ are the components of $\mathbf{r}$ parallel to the plate and $T_{zz}=\frac{1}{2}(\partial_z\phi)^2-\frac{1}{2}\left[(\partial_x\phi)^2+(\partial_y\phi)^2\right]$ is the zz-component of the stress tensor [6,56] (see text below Eq. (104) in Ref. [56] for a discussion of the stress tensor in connection with critical dynamics). Similarly, the force per unit area acting on the other side of plate 1 is given by $F_-/A=-\lim_{z\to 0}\langle T_{zz}(\mathbf{r}_\parallel,z,t)\rangle_{L=\infty}$ where T_{zz} is again evaluated in the cavity between the plates but for the limit $L\to\infty$ (see Fig. 1). The net force per unit area on plate 1 yields as

$$\frac{F(t)}{A}=\lim_{z\to 0}\langle T_{zz}(\mathbf{r}_\parallel,z,t)\rangle-\lim_{z\to 0}\langle T_{zz}(\mathbf{r}_\parallel,z,t)\rangle_{L=\infty}. \tag{6}$$

Using the Dirichlet boundary condition $\phi=0$ at the plates we obtain

$$\lim_{z\to 0}\langle T_{zz}(\mathbf{r}_\parallel,z,t)\rangle=\frac{1}{2}\lim_{z,z'\to 0}\partial_z\partial_{z'}\langle\phi(\mathbf{r}_\parallel,z,t)\phi(\mathbf{r}_\parallel,z',t)\rangle. \tag{7}$$

To calculate the two-point correlation function of ϕ on the right-hand side of Eq. (7) we note that the solution $\phi(\mathbf{r},t)$ of Eq. (4) can be expressed as

$$\phi(\mathbf{r},t)=\int_{-\infty}^{\infty}dt'\int_{V(t')}d^3\mathbf{r}'G(\mathbf{r},t;\mathbf{r}',t')\eta(\mathbf{r}',t') \tag{8}$$

where $V(t')=A\cdot L(t')$ is the volume of the cavity at time t' and the Green's function $G(\mathbf{r},t;\mathbf{r}',t')$ is defined as the solution of

$$\left(\gamma\frac{\partial}{\partial t}-\nabla_r^2\right)G(\mathbf{r},t;\mathbf{r}',t')=\delta^{(3)}(\mathbf{r}-\mathbf{r}')\delta(t-t') \tag{9}$$

subject to the boundary condition $G(\mathbf{r},t;\mathbf{r}',t')=0$ whenever $\mathbf{r}$ or $\mathbf{r}'$ is located on the surface of one of the plates (note that $G(\mathbf{r},t;\mathbf{r}',t')$ is symmetric in $\mathbf{r}$ and $\mathbf{r}'$). In addition, $G(\mathbf{r},t;\mathbf{r}',t')=0$ for $t'>t$ by causality. Thus, $\phi(\mathbf{r},t)$ can be expressed as a linear superposition of contributions from the source $\eta(\mathbf{r}',t')$ at times $t'<t$ and positions $\mathbf{r}'\in V(t')$, carried forward in time by the propagator $G(\mathbf{r},t;\mathbf{r}',t')$. Using Eqs. (8) and (5) one finds the two-point correlation function

$$\langle\phi(\mathbf{r},t)\phi(\mathbf{r}',t')\rangle=2\gamma k_BT\int_{-\infty}^{\infty}ds\int_{V(s)}d^3x\,G(\mathbf{r},t;x,s)G(\mathbf{r}',t';x,s). \tag{10}$$

In the present set-up, the system is translationally invariant in xy-direction at any time t, whereas translation invariance in time is broken due to the varying separation $L(t)$ between the plates. Thus, introducing the partial Fourier transform g of G as

$$G(\mathbf{r}_\parallel,z,t;\mathbf{r}'_\parallel,z',t')=\int\frac{d^2p}{(2\pi)^2}e^{ip\cdot(\mathbf{r}_\parallel-\mathbf{r}'_\parallel)}\int_{-\infty}^{\infty}\frac{d\omega}{2\pi}e^{-i\omega(t-t')}g(z,z';\omega,p,t'), \tag{11}$$

the function g depends explicitly on one of the time coordinates in G, say, t'. Using Eqs. (10), (11) we find for the expression in Eq. (7) (the star symbol indicates the complex conjugate for real-valued argument ω)

$$\lim_{z\to 0}\langle T_{zz}(\mathbf{r}_\parallel,z,t)\rangle=\gamma k_BT\int\frac{d^2p}{(2\pi)^2}\int_{-\infty}^{\infty}\frac{d\omega}{2\pi}\int_0^{L(t)}d\zeta\,u(\zeta,\omega,p,t)u^*(\zeta,\omega,p,t) \tag{12}$$

where

$$u(\zeta,\omega,p,t)=\frac{\partial}{\partial z}g(z,\zeta;\omega,p,t)|_{z=0}. \tag{13}$$

For given propagator G, hence function u, $F(t)/A$ is obtained using Eqs. (6) and (12) (cf. Methods).

Diffusion of Stress and Resonant Dissipation

The ratio $F(t)/F_0$ of the fluctuation-induced, time-dependent force $F(t)$ on plate 1 due to the vibrating plate 2 and the corresponding static force F_0 is a universal (cutoff-independent) function of a/L_0 (geometry), ω_0t (time-dependence of the driving), and the dimensionless parameter

$$\Omega=\omega_0\gamma L_0^2 \tag{14}$$

(see Eqs. (1), (3), (4), and Fig. 1). Our results for $F(t)/F_0$ correspond to an expansion to first order in $a/L_0\ll 1$ and can be cast in the form

$$\frac{F(t)}{F_0}=1-\frac{3a}{L_0}f(\omega_0t,\Omega)+\mathcal{O}\left[(a/L_0)^2\right] \tag{15a}$$

where the dimensionless function $f(\omega_0t,\Omega)$ is normalized such that $f=1$ for $\omega_0=0$. For $\omega_0>0$ the function $f(\omega_0t,\Omega)$ can be represented as

$$f(\omega_0t,\Omega)=\Phi(\Omega)\cos[\omega_0t-\varphi(\Omega)] \tag{15b}$$

in terms of an amplitude $\Phi(\Omega)$ and a phase shift $\varphi(\Omega)$.

The amplitude $\Phi(\Omega)$ is shown in Fig. 2. For $\Omega=0$, i.e., $\omega_0=0$, the normalization $f(0,0)=1$ in conjunction with $\varphi(0)=0$ (see below) implies $\Phi(0)=1$. For $\Omega>0$, i.e., $\omega_0>0$, the length $l=(\omega_0\gamma)^{-1/2}$ is a measure of the distance over which a perturbation diffuses during an oscillation. For increasing $\Omega=L_0^2/l^2$ a variation of stress generated at the vibrating plate 2 is more and more attenuated, i.e., washed out, due to the diffusive nature of the medium before it reaches plate 1; thus $\Phi(\Omega)$ is monotonically decreasing for increasing Ω (Fig. 2, black line).

The force $F(t)$ in Eq. (15) has contributions of different physical origin related to diffusion of stress (dif) and resonant dissipation (res) in the medium between the plates, i.e.,

$$F(t)=F_{\rm dif}(t)+F_{\rm res}(t). \tag{16}$$

The contributions $F_{\rm dif}(t)$ and $F_{\rm res}(t)$ are related to real and imaginary poles in the complex-frequency plane occurring in the calculation of $F(t)$, respectively (see Eqs. (35) and (37)). Both $F_{\rm dif}(t)$ and $F_{\rm res}(t)$ may be expanded as in Eq. (15):

$$\frac{F_{\rm dif}(t)}{F_0}=1-\frac{3a}{L_0}f_{\rm dif}(\omega_0t,\Omega)+\mathcal{O}\left[(a/L_0)^2\right], \tag{17a}$$

$$f_{\rm dif}(\omega_0t,\Omega)=\Phi_{\rm dif}(\Omega)\cos[\omega_0t-\varphi_{\rm dif}(\Omega)], \tag{17b}$$

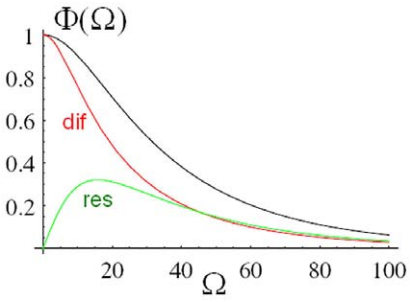

Figure 2. Amplitude of the non-equilibrium Casimir force. Amplitude $\Phi(\Omega)$ of $f(\omega_0 t,\Omega)$ as a function of $\Omega=\omega_0\gamma L_0^2$ (see Eq. (15)) (black line). Also shown are the amplitudes $\Phi_{\rm dif}(\Omega)$ of $f_{\rm dif}(\omega_0 t,\Omega)$ (dif, red line) and $\Phi_{\rm res}(\Omega)$ of $f_{\rm res}(\omega_0 t,\Omega)$ (res, green line) describing contributions to $F(t)$ due to diffusion of stress and resonant dissipation, respectively (see Eqs. (17), (18)).
doi:10.1371/journal.pone.0053228.g002

and

$$\frac{F_{\rm res}(t)}{F_0}=1-\frac{3a}{L_0}f_{\rm res}(\omega_0 t,\Omega)+\mathcal{O}\left[(a/L_0)^2\right], \qquad (18a)$$

$$f_{\rm res}(\omega_0 t,\Omega)=\Phi_{\rm res}(\Omega)\cos[\omega_0 t-\varphi_{\rm res}(\Omega)]. \qquad (18b)$$

The amplitude $\Phi_{\rm dif}(\Omega)$ is shown as the red line in Fig. 2. For $\Omega=0$, i.e., $\omega_0=0$, there is no contribution from resonant dissipation, thus $\Phi_{\rm res}(0)=0$ and $\Phi_{\rm dif}(0)=\Phi(0)=1$ (however, $\Phi(\Omega)\neq\Phi_{\rm dif}(\Omega)+\Phi_{\rm res}(\Omega)$ for $\Omega>0$ because $\varphi_{\rm dif}(\Omega)\neq\varphi_{\rm res}(\Omega)$). For $\Omega>0$ the amplitude $\Phi_{\rm dif}(\Omega)$ is attenuated due to the diffusive nature of the medium as discussed in relation to $\Phi(\Omega)$ above; thus $\Phi_{\rm dif}(\Omega)=1$ is monotonically decreasing for increasing Ω (Fig. 2, red line). Finally, the amplitude $\Phi_{\rm res}(\Omega)$ due to resonant dissipation is shown as the green line in Fig. 2. Resonant dissipation is absent in the static case $\omega_0=0$, i.e., $\Omega=0$, which implies $\Phi_{\rm res}(0)=0$. For large Ω the amplitude $\Phi_{\rm res}(\Omega)$ is attenuated due to the diffusive nature of the medium as discussed in relation to $\Phi(\Omega)$ above; thus $\Phi_{\rm res}(\Omega)$ starts at $\Phi_{\rm res}(0)=0$, is increasing for small Ω and monotonically decreasing for large Ω (Fig. 2, green line).

Figure 3 shows the phase shift $\varphi(\Omega)$ of the function $f(\omega_0 t,\Omega)$ in Eq. (15b) in terms of the variable $\tau(\Omega)=\varphi(\Omega)/\Omega$. Thus, using Eq. (14), $\varphi(\Omega)=\Omega\tau(\Omega)\equiv\omega_0 t_l(\Omega)$, where the lag time $t_l(\Omega)=\gamma L_0^2\tau(\Omega)$ is a measure of the time a variation of stress generated at the vibrating plate 2 takes to diffuse through the medium to reach plate 1. For illustration, for $\omega_0=2\pi\,{\rm s}^{-1}$ and $\Omega=10$ we obtain $t_l=\tau(\Omega)\Omega/\omega_0\simeq 0.15\,{\rm s}$. $t_l(\Omega)$ is fairly constant over a wide range of Ω and approaches a finite value $t_l(0)$ for $\Omega\to 0$ (Fig. 3a, black line); thus $t_l\sim L_0^2$ as expected for the present diffusive dynamics in the medium between the plates. In the limit $\Omega\to 0$ the relation $\varphi(\Omega)=\Omega\tau(\Omega)$ with finite $\tau(0)$ implies $\varphi(\Omega)\to 0$. A qualitatively similar behavior occurs for the phase shift $\varphi_{\rm dif}(\Omega)$ of the function $f_{\rm dif}(\omega_0 t,\Omega)$ in Eq. (17b) (Fig. 3a, red line). Finally, Fig. 3b shows the phase shift $\varphi_{\rm res}(\Omega)$ of the function $f_{\rm res}(\omega_0 t,\Omega)$ in Eq. (18b); in this case, $\varphi_{\rm res}(\Omega)$ itself is approximately constant and approaches a finite value for $\Omega\to 0$ (in contrast to $\varphi(\Omega)$, for which $\varphi(\Omega)/\Omega$ is approximately constant, see above). This implies that the corresponding lag time $t_{l,{\rm res}}(\Omega)=\gamma L_0^2\varphi_{\rm res}(\Omega)/\Omega$ formally diverges for $\Omega\to 0$, i.e., $\omega_0\to 0$, which reflects the fact that resonant dissipation is absent in the static case $\omega_0=0$. However, the divergence of $t_{l,{\rm res}}(\Omega)$ for $\Omega\to 0$ is suppressed in the net force $F(t)$ since the amplitude $\Phi_{\rm res}(\Omega)$ in Eq. (18b) vanishes for $\Omega\to 0$, so that the lag time $t_l(\Omega)$ of $F(t)$ stays finite for $\Omega\to 0$ (see Eq. (15) and Fig. 3a).

Discussion

We have studied the fluctuation-induced, time-dependent force $F(t)$ between two plates confining a fluid which is driven out of equilibrium mechanically by harmonic oscillations of one of the plates, assuming purely relaxational dynamics of the fluid (corresponding to the critical dynamics of model A [51,52]) (see Fig. 1). Our main results for $F(t)$, valid to first order in the amplitude a of the oscillations, are summarized in Figs. 2 and 3. We find two distinct contributions to $F(t)$ related to diffusion of stress in the fluid and resonant dissipation, respectively. Resonant dissipation has been studied for the dynamic Casimir effect of the electromagnetic field, where it is a result of enhanced creation of photons if the driving frequency corresponds to a resonance frequency of the cavity [41–44]. In the present case, dissipation is generated by the viscosity of the fluid described by the friction parameter γ in the Langevin equation (4).

Fluctuation-induced forces may be observed, e.g., by means of atomic force microscopy (AFM). To avoid the experimental difficulty of keeping two flat plates parallel one usually employs geometries in which one of the surfaces is curved; for example, by measuring the force between a sphere attached to the tip of an AFM cantilever and a flat plate. The force $F_s(L_0)$ on a sphere of radius R separated by a distance L_0 surface-to-surface from a flat plate is related to the energy of interaction per surface area $\varepsilon(L_0)$ between two flat plates by the proximity force rule $F_s(L_0)=2\pi R\varepsilon(L_0)$. For example, the static force per unit area F_0/A in Eq. (3) yields $F_s(L_0)=-\zeta(3)Rk_BT/(8L_0^2)=-6.2$ PT for $T=300$ K, $R=100\mu$m, $L_0=100$ nm, which is readily accessible by AFM.

Fluctuation-induced forces between moving objects are expected to occur for any medium exhibiting long-ranged correlations. However, as mentioned in the Introduction, for real fluids the model needs to be modified to take into account conservation of the order parameter and its convection with the transverse momentum current of the fluid, thus treating Casimir and hydrodynamic interactions on the same footing (corresponding to the critical dynamics of model H [53]); these effects are important and will modify the result for $F(t)$ in Eq. (15) obtained for the purely relaxational dynamics of model A (see [51,52] for reviews on dynamic critical behavior and its comparison with experiments). However, the time-dependent force $F(t)$ predicted in Eq. (15) may be observable by means of computer simulations of the ferromagnetic Ising model (or corresponding lattice gas models) confined between two plates, one of which is vibrating at small amplitude.

A much-studied subject related to the present study are hydrodynamic interactions of microscopic objects in viscous fluids since they are relevant, e.g., to the motility and locomotion of swimming microorganisms [57]. Recently, motivated by devices such as the AFM, the drag experienced by a cylindrical object (modeling an AFM cantilever) and a sphere oscillating at small amplitude near a flat surface were studied in detail [58,59]; however, few results are available concerning the hydrodynamic force generated by an oscillating object on a *different* object nearby. Thus, it would be interesting to probe effective hydrodynamic interactions between different, moving objects immersed in a viscous fluid, and how these interactions are modified by the Casimir force when correlations in the fluid become long-ranged.

The fluctuation-induced, time-dependent force $F(t)$ on plate 1 due to the vibrating plate 2 is universal in the sense that it is largely

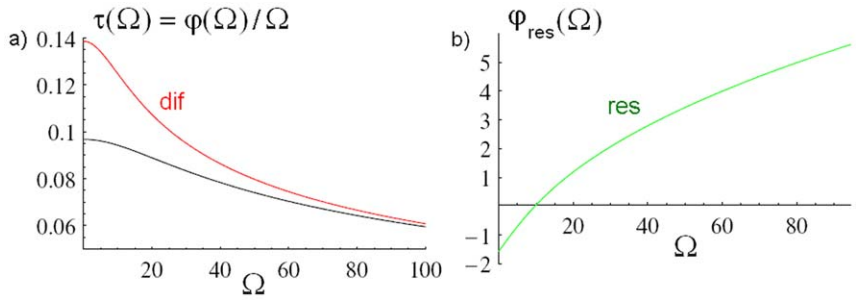

Figure 3. Phase shift of the non-equilibrium Casimir force. (a) Phase shift $\varphi(\Omega)$ of $f(\omega_0 t,\Omega)$ in terms of $\tau(\Omega)=\varphi(\Omega)/\Omega$ (see Eq. (15)) (black line). Also shown is the phase shift $\varphi_{\rm dif}(\Omega)$ of $f_{\rm dif}(\omega_0 t,\Omega)$ describing the contribution to $F(t)$ due to diffusion of stress (dif, red line) (see Eq. (17)). (b) Phase shift $\varphi_{\rm res}(\Omega)$ of $f_{\rm res}(\omega_0 t,\Omega)$ describing the contribution to $F(t)$ due to resonant dissipation (res) (see Eq. (18)).
doi:10.1371/journal.pone.0053228.g003

independent of microscopic details of the system. The force ratio $F(t)/F_0$, where F_0 is the force at fixed separation L_0, only depends on the dimensionless variables a/L_0 (geometry), $\omega_0 t$ (time-dependence of the driving), and $\Omega=\omega_0\gamma L_0^2$ characterizing the viscosity of the fluid. It would be interesting to generalize our approach to the electromagnetic field to study the analogous, time-dependent Casimir force $F(t)$ for the dynamic Casimir effect of the electromagnetic field.

Methods

The Propagator G

The calculation of the non-equilibrium Casimir force $F(t)$ by Eqs. (6) and (12) requires the propagator $G(\mathbf{r},t;\mathbf{r}',t')$ solving Eq. (9) subject to the time-dependent boundary conditions due to the vibrating plate 2. This problem can be solved, for general modulations of the plate(s) in space and time, by the method developed in Refs. [60,61]. For the present set-up, we find for the partial Fourier transform $\mathcal{G}(z,t;z',t';p)$ of G (i.e., transforming the spatial coordinates $\mathbf{r}_\parallel$, $\mathbf{r}'_\parallel$ parallel to the plates as in Eq. (11) but keeping the time coordinates t, t'; in what follows, we omit the argument p for ease of notation) [60,61]

$$\mathcal{G}(z,t;z',t')=\overline{\mathcal{G}}(z,t;z',t')-\int_{-\infty}^{\infty}d\tau\int_{-\infty}^{\infty}d\sigma\,\overline{\mathcal{G}}[z,t;L(\tau),\tau]\,M(\tau,\sigma)\overline{\mathcal{G}}[L(\sigma),\sigma;z',t'] \tag{19}$$

where $\overline{\mathcal{G}}$ is the propagator in the half-space $z>0$ bounded by a Dirichlet surface at $z=0$ (that is, the function $\overline{\mathcal{G}}$ itself is independent of the vibrating plate 2; the dependence of $\mathcal{G}$ on plate 2 in Eq. (19) only enters through the arguments $L(\tau)$, $L(\sigma)$ in $\overline{\mathcal{G}}$, and the kernel $M(\tau,\sigma)$). The kernel M is defined by

$$\int_{-\infty}^{\infty}d\sigma\,M(\tau,\sigma)\overline{\mathcal{G}}[L(\sigma),\sigma;L(t),t]=\delta(\tau-t). \tag{20}$$

In this work, we consider small variations of the separation between the plates about a mean separation L_0, i.e.,

$$L(t)=L_0+h(t). \tag{21}$$

Our results hold to first order in h. To this end, we insert Eq. (21) in Eq. (19) and expand everything to first order in h (note that $L(t)=L_0+h(t)$ also enters the upper boundary of the integration over ζ in Eq. (12)). This results in expansions $g=g_0+g_1+\mathcal{O}(h^2)$ and $u=u_0+u_1+\mathcal{O}(h^2)$ of the functions g and u from Eqs. (11), (13) in powers of h. Equations (6), (12) then yield the corresponding contributions to $F(t)/A$.

Let us first consider the leading order, i.e., $h=0$ and $L(t)=L_0$. Using Eq. (19) and transforming to ω-space as in Eq. (11) we find (omitting the arguments p and ω for ease of notation)

$$g_0(z,z')=\bar{g}(z,z')-\bar{g}(z,L_0)\,M_0\,\bar{g}(L_0,z') \tag{22}$$

where $\bar{g}(z,z')=\left[e^{-Q|z-z'|}-e^{-Q(z+z')}\right]/(2Q)$ with $Q=\sqrt{p^2-i\gamma\omega}$ from Eq. (26) below and $M_0=[\bar{g}(L_0,L_0)]^{-1}=2Q/[1-\exp(-2QL_0)]$. Thus,

$$g_0(z,z')=\frac{\sinh(Qz)\sinh[Q(L_0-z')]}{Q\sinh(QL_0)},\ z<z', \tag{23}$$

and, using Eq. (13),

$$u_0(\zeta)=\frac{\partial}{\partial z}g_0(z,\zeta)|_{z=0}=\frac{\sinh[Q(L_0-\zeta)]}{\sinh(QL_0)}. \tag{24}$$

Using Eqs. (6), (12), (24) we thus obtain to leading order [31]

$$\frac{F_0}{A}=-\frac{k_BT}{2}\int\frac{d^2p}{(2\pi)^2}\int_{-\infty}^{\infty}\frac{d\omega}{2\pi i}\,\frac{1}{\omega+i\varepsilon}\,(Q[\coth(QL_0)-1]-P[\coth(PL_0)-1]) \tag{25a}$$

$$=-\frac{k_BT}{2}\int\frac{d^2p}{(2\pi)^2}\,p[\coth(pL_0)-1]. \tag{25b}$$

The integral in Eq. (25b) is finite and yields Eq. (3). In Eq. (25a) we use

$$Q(\omega,p)=\sqrt{p^2-i\gamma\omega},P(\omega,p)=\sqrt{p^2+i\gamma\omega}, \tag{26}$$

so that $P=Q^*$ if ω is real. Integrations over ω as in Eq. (25a) are readily computed by contour integration in the complex ω-plane. In Eq. (25a) and throughout this work we use the convention that in ω-integrations we integrate *above* the pole in ω; this can be

accomplished by the replacement $\omega\to\omega+i\varepsilon$ in the denominator of the integrand in Eq. (25a). The limit $\varepsilon\to 0$ in final results is always understood. Note that this prescription introduces a positive time direction and ensures causality. $Q(\omega)$ has a branch cut along the negative imaginary axis $\gamma\omega=-i(p^2+r)$, $r\geq 0$, whereas $P(\omega)$ has a branch cut along the positive imaginary axis $\gamma\omega=i(p^2+r)$, $r\geq 0$. The integral over ω in Eq. (25a) has two contributions. For the contribution involving $Q[\coth(QL_0)-1]$, the contour integral can be closed in the upper complex ω-plane (thus avoiding the branch cut of Q), where this term has no poles, so that the contribution from this term vanishes. Likewise, for the contribution involving $P[\coth(PL_0)-1]$, the contour integral can be closed in the lower complex ω-plane (avoiding the branch cut of P), where, in turn, this term has no poles. The single pole at $\omega=-i\varepsilon$ in the lower complex ω-plane then yields the expression in Eq. (25b); cp. Fig. 4a with $\omega_0=0$.

We now turn to the contribution to $F(t)/A$ to first order in h. Using the expansion

$$u(\zeta;\omega,p,t)=u_0(\zeta;\omega,p)+u_1(\zeta;\omega,p,t)+\mathcal{O}(h^2) \tag{27}$$

in Eq. (12), with u from Eq. (13) and u_0 from Eq. (24), we find for general $h(t)$

$$\frac{F_1(t)}{A}=\frac{k_BT}{2}\int\frac{d^2p}{(2\pi)^2}\int_{-\infty}^{\infty}\frac{d\omega}{2\pi}[f(\omega,p,t)+f^*(\omega,p,t)] \tag{28}$$

where

$$f(\omega,p,t)=\frac{Q}{\sinh(QL_0)}\overset{h}{\circ}\frac{1}{i\omega}\left[\frac{Q}{\sinh(QL_0)}-\frac{P}{\sinh(PL_0)}\right]. \tag{29}$$

The symbol $\overset{h}{\circ}$ denotes a convolution of two functions $\hat{a}(\omega)$, $\hat{b}(\omega)$ involving an insertion of $h(t)=\int_{-\infty}^{\infty}\frac{d\omega}{2\pi}\exp(-i\omega t)\hat{h}(\omega)$:

$$(\hat{a}\overset{h}{\circ}\hat{b})(\omega,t')=\hat{a}(\omega)\int_{-\infty}^{\infty}\frac{d\omega'}{2\pi}e^{-i(\omega-\omega')t'}\hat{h}(\omega-\omega')\hat{b}(\omega'). \tag{30}$$

For functions $a(t,t')$, $b(t,t')$, the expression $(\hat{a}\overset{h}{\circ}\hat{b})(\omega,t')$ is the representation in ω-space of $c(t,t'):=\int_{-\infty}^{\infty}ds\,a(t,s)h(s)b(s,t')$; i.e., $c(t,t')=\int_{-\infty}^{\infty}\frac{d\omega}{2\pi}\exp[-i\omega(t-t')](\hat{a}\overset{h}{\circ}\hat{b})(\omega,t')$. The functions $\hat{a}(\omega)$, $\hat{b}(\omega)$ are the representations in ω-space of $a(t,s)$, $b(s,t')$, respectively. Equations (28), (29) are obtained by using Eq. (19) with $L(t)=L_0+h(t)$, expanding everything to first order in h, and using Eq. (30) for the resulting insertions of $h(t)$. The contribution of M to first order in h is determined by Eq. (20), resulting in $M_1=-M_0\bar{g}_1M_0$ where the subscripts 0 and 1 indicate the order in h; M_0 is given below Eq. (22).

For the special case that plate 2 is vibrating with harmonic oscillations of amplitude a and frequency ω_0 (see Eqs. (1), (21)), i.e.,

$$h(t)=a\cos(\omega_0 t), \tag{31}$$

we obtain $\hat{h}(\omega)=a\pi[\delta(\omega-\omega_0)+\delta(\omega+\omega_0)]$. The integral $\int_{-\infty}^{\infty}\frac{d\omega}{2\pi}(f+f^*)$ in Eq. (28) decays into two contributions corresponding to the terms in square brackets on the right-hand side of Eq. (29):

$$\int_{-\infty}^{\infty}\frac{d\omega}{2\pi}[f(\omega,p,t)+f^*(\omega,p,t)]=\Phi_{QQ}(p,t)+\Phi_{QP}(p,t), \tag{32}$$

where the subscripts QQ and QP indicate the contributions from the first and second term in square brackets of Eq. (29), respectively. In what follows we show that these two terms yield distinct contributions to $F(t)$ corresponding to real-valued and imaginary poles in the complex ω-plane.

Real-Valued Frequency Poles: Diffusion of Stress and Finite Lag Time

For the first contribution in Eq. (32) we find (the *c.c.* symbol indicates the complex conjugate of the preceding expression; regarding the replacement $\omega\to\omega+i\varepsilon$ in the denominator of the integrand, see the discussion below Eq. (26))

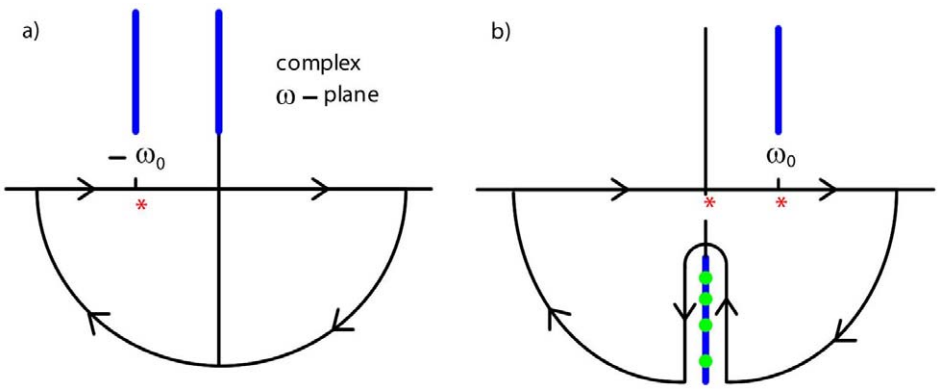

Figure 4. Contour integration in the complex ω-plane. (a) Contour integration for the second term in square brackets in Eq. (33). The only contribution from this term is from the pole at $\omega=-\omega_0-i\varepsilon$ indicated by the red star. The blue lines indicate branch cuts of $v(\omega)v(\omega+\omega_0)$. (b) Contour integration in Eq. (36). The blue lines indicate branch cuts of of $u(\omega)v(\omega-\omega_0)$. The contributions from the poles at $\omega=\omega_0-i\varepsilon$ and $\omega=-i\varepsilon$ cancel (see text).
doi:10.1371/journal.pone.0053228.g004

$$\Phi_{QQ}(p,t)=\frac{a}{2}\,e^{-i\omega_0 t}\int_{-\infty}^{\infty}\frac{d\omega}{2\pi i}\left[\frac{u(\omega)u(\omega-\omega_0)}{\omega-\omega_0+i\varepsilon}-\frac{v(\omega)v(\omega+\omega_0)}{\omega+\omega_0+i\varepsilon}\right]+c.c. \tag{33}$$

where

$$u(\omega)=\frac{Q}{\sinh(QL_0)},v(\omega)=\frac{P}{\sinh(PL_0)}, \tag{34}$$

with Q, P from Eq. (26). Computing the right-hand side of Eq. (33) by contour integration in the complex ω-plane, the contributions from the two terms in square brackets in the integrand are analyzed along similar lines as discussed below Eq. (26). Thus, for the first term in square brackets, the contour integral can be closed in the upper complex ω-plane, where $u(\omega)$ has no poles, so that the contribution from this term vanishes. For the second term in square brackets, the contour integral can be closed in the lower complex ω-plane, where $v(\omega)$ has no poles. The only contribution from this term is from the single pole at $\omega=-\omega_0-i\varepsilon$; see Fig. 4a. Thus, including the contribution from the complex conjugate in Eq. (33), we obtain

$$\Phi_{QQ}(p,t)=\frac{ap}{2\sinh(pL_0)}\left[e^{i\omega_0 t}v(\omega_0)+e^{-i\omega_0 t}u(\omega_0)\right]. \tag{35}$$

The corresponding contribution to $F_1(t)/A$ is given by $\frac{k_BT}{2}\int\frac{d^2p}{(2\pi)^2}\Phi_{QQ}(p,t)$ (see Eqs. (28) and (32)). In the static case, where $\omega_0=0$ and $h(t)=a$ in Eq. (1), this result can also be obtained directly from Eq. (25b) by replacing L_0 with L_0+a and expanding to first order in a. For finite ω_0, Eq. (35) emerges from the static case by a shift from $\omega_0=0$ to a finite value of ω_0. This shift may be understood in terms of a transition from stationary modes in the cavity in the static case to modes with a time-dependence $\sim\exp(i\omega_0 t)$ in response to the vibrating plate 2. The resulting fluctuation-induced force $F(t)$ on plate 1 is characterized by a finite lag time t_l which is a measure of the time a variation of stress in the medium generated at the vibrating plate 2 takes to diffuse through the medium to reach plate 1 (see Fig. 1). For the present diffusive dynamics, t_l is related to the distance L_0 between the plates by $t_l\sim L_0^2$.

Imaginary Frequency Poles: Resonant Dissipation

For the second contribution in Eq. (32) we find

$$\Phi_{QP}(p,t)=-\frac{a}{2}\,e^{-i\omega_0 t}\omega_0\int_{-\infty}^{\infty}\frac{d\omega}{2\pi i}\left[\frac{u(\omega)v(\omega-\omega_0)}{(\omega-\omega_0+i\varepsilon)(\omega+i\varepsilon)}\right]+c.c. \tag{36}$$

The contour integral over ω can be closed either in the upper or the lower complex ω-plane, yielding identical results; the contributions from the poles at $\omega=\omega_0-i\varepsilon$ and $\omega=-i\varepsilon$ in the lower complex ω-plane cancel. Closing the contour integral in the lower plane, the integral picks up contributions from the imaginary poles $\gamma\omega_n=-i(p^2+k_n^2)$ of $u(\omega)$, where $k_n=n\pi/L_0$ and $n\geq 1$ is a positive integer. Note that $u(\omega)$ has a branch cut along the negative imaginary axis on which the poles ω_n are located (see the related discussion below Eq. (26)); however, this branch cut may be cured using the identity $Q/\sinh(QL_0)=R/\sin(RL_0)$, with $R(\omega,p)=\sqrt{i\gamma\omega-p^2}$, which holds close to the negative imaginary axis. The expression $R/\sin(RL_0)$ is analytic in the lower complex ω-plane with isolated poles at ω_n; see Fig. 4b. Summing over the residues of these poles yields

$$\Phi_{QP}(p,t)=a\,e^{-i\omega_0 t}\,\frac{i\gamma\omega_0}{L_0}\sum_{n=1}^{\infty}(-1)^n\frac{v(\omega_n-\omega_0)k_n^2}{(p^2+k_n^2)(p^2+k_n^2-i\gamma\omega_0)}+c.c. \tag{37}$$

The corresponding contribution to $F_1(t)/A$ is given by $\frac{k_BT}{2}\int\frac{d^2p}{(2\pi)^2}\Phi_{QP}(p,t)$. Note that $\Phi_{QP}(p,t)$ is proportional to ω_0, which implies that this term is absent in the static case $\omega_0=0$ and solely generated by the fact that the system is driven out of equilibrium by the vibrating plate 2 (see Fig. 1). The imaginary-frequency poles $\gamma\omega_n=-i(p^2+k_n^2)$ leading to Eq. (37) are related to resonant dissipation in the cavity, where the spectrum of imaginary resonance frequencies ω_n is continuous due to the presence of the continuous in-plane wave number p (compare the related discussion of resonant dissipation in the context of the dynamic Casimir effect of the electromagnetic field in Ref. [43]). Resonant dissipation has been studied for the dynamic Casimir effect of the electromagnetic field, where it is a result of enhanced creation of photons if the driving frequency corresponds to a resonance frequency of the cavity [41–44].

Author Contributions

Analyzed the data: AH. Contributed reagents/materials/analysis tools: AH. Wrote the paper: AH.

References

1. McMullin E (2002) The origins of the field concept in physics. Phys Perspect 4: 13–39.
2. Collins H (2004) Gravity's Shadow: The Search For Gravitational Waves. Chicago: University of Chicago Press.
3. Casimir HBG (1948) On the attraction between two perfectly conducting plates. Proc K Ned Akad Wet 51: 793–795.
4. Milonni PW (1993) The Quantum Vacuum: An Introduction to Quantum Electrodynamics. San Diego: Academic.
5. Golestanian R, Kardar M (1999) The "friction" of vacuum, and other fluctuation-induced forces. Rev Mod Phys 71: 1233–1245.
6. Milton KA (2001) The Casimir Effect. Singapore: World Scientific.
7. Bordag M, Klimchitskaya GL, Mohideen U, Mostepanenko VM (2009) Advances in the Casimir Effect. Oxford: Oxford University Press.
8. Lamoreaux SK (1997) Demonstration of the casimir force in the 0.6 to 6 m range. Phys Rev Lett 78: 5–8.
9. Mohideen U, Roy A (1998) Precision measurement of the casimir force from 0.1 to 0.9 m. Phys Rev Lett 81: 4549–4552.
10. Chan HB, Aksyuk VA, Kleiman RN, Bishop DJ, Capasso F (2001) Quantum mechanical actuation of microelectromechanical systems by the casimir force. Science 291: 1941–1944.
11. Chan HB, Aksyuk VA, Kleiman RN, Bishop DJ, Capasso F (2001) Nonlinear micromechanical casimir oscillator. Phys Rev Lett 87: 211801–211804.
12. Capasso F, Munday JN, Iannuzzi D, Chan HB (2007) Casimir forces and quantum electrodynamical torques: Physics and nanomechanics. IEEE J Sel Top Quantum Electron 13: 400–414.
13. Sushkov AO, Kim WJ, Dalvit DAR, Lamoreaux SK (2011) Observation of the thermal casimir force. Nature Phys 7: 230–233.
14. Emig T, Hanke A, Golestanian R, Kardar M (2001) Probing the strong boundary shape dependence of the casimir force. Phys Rev Lett 87: 260402–260405.
15. Emig T, Hanke A, Golestanian R, Kardar M (2003) Normal and lateral casimir forces between deformed plates. Phys Rev A 67: 022114–022128.
16. Gies H, Klingmüller K (2006) Casimir edge effects. Phys Rev Lett 97: 220405–220408.

17. Canaguier-Durand A, Neto PAM, Cavero-Pelaez I, Lambrecht A, Reynaud S (2009) Casimir interaction between plane and spherical metallic surfaces. Phys Rev Lett 102: 230404–230407.
18. Emig T (2009) Casimir forces and geometry in nanosystems. In: Radons G, Rumpf B, Schuster HG, editors, Nonlinear Dynamics of Nanosystems, New York: Wiley, chapter 6.
19. Reid MTH, Rodriguez AW, White J, Johnson SG (2009) Efficient computation of casimir interactions between arbitrary 3 d objects. Phys Rev Lett 103: 040401–040404.
20. Rodriguez AW, McCauley AP, Joannopoulos JD, Johnson SG (2009) Casimir forces in the time domain: Theory. Phys Rev A 80: 012115–012125.
21. Bordag M, Nikolaev V (2009) Beyond proximity force approximation in the casimir effect. Int J Mod Phys A 24: 1743–1747.
22. Krech M (1994) The Casimir Effect in Critical Systems. Singapore: World Scientific.
23. Li H, KardarM (1992) Fluctuation-induced forces between manifolds immersed in correlated fluids. Phys Rev A 46: 6490–6500.
24. Fisher ME, de Gennes PG (1978) Phnomnes aux parois dans un mlange binaire critique. C R Acad Sci (Paris) 287: 207–209.
25. Hertlein C, Helden L, Gambassi A, Dietrich S, Bechinger C (2008) Direct measurement of critical casimir forces. Nature 451: 172–175.
26. Hanke A, Schlesener F, Eisenriegler E, Dietrich S (1998) Critical casimir forces between spherical particles in fluids. Phys Rev Lett 81: 1885–1888.
27. Schlesener F, Hanke A, Dietrich S (2003) Critical casimir forces in colloidal suspensions. J Stat Phys 110: 981–1013.
28. Vasilyev O, Gambassi A, Maciolek A, Dietrich S (2009) Universal scaling functions of critical casimir forces obtained by monte carlo simulations. Rev Rev E 79: 041142–041162.
29. Emig T (2007) Casimir-force-driven ratchets. Phys Rev Lett 98: 160801–160804.
30. Bartolo D, Ajdari A, Fournier JB (2003) Effective interactions between inclusions in complex fluids driven out of equilibrium. Phys Rev E 67: 061112–061120.
31. Najafi A, Golestanian R (2004) Forces induced by nonequilibrium fluctuations: The soret-casimir effect. EPL 68: 776–782.
32. Dean DS, Gopinathan A (2009) The non-equilibrium behavior of fluctuation induced forces. J Stat Mech: Theory Exp 81: L08001-L08008.
33. Dean DS, Gopinathan A (2010) Out–of-equilibrium behavior of casimir-type fluctuation-induced forces for free classical fields. Phys Rev E 81: 041126–041136.
34. Demery V, Dean DS (2010) Drag forces in classical fields. Phys Rev Lett 104: 080601–080604.
35. Demery V, Dean DS (2011) Thermal casimir drag in fluctuating classical fields. Phys Rev E 84: 010103–010106.
36. Cattuto C, Brito R, Marconi UMB, Nori F, Soto R (2006) Fluctuation-induced casimir forces in granular fluids. Phys Rev Lett 96: 178001–178004.
37. Brito R, Marconi UMB, Soto R (2007) Generalized casimir forces in nonequilibrium systems. Phys Rev E 76: 011113–011117.
38. Buenzli PR, Soto R (2008) Violation of the action-reaction principle and self-forces induced by nonequilibrium fluctuations. Phys Rev E 78: 020102–020105.
39. Rodriguez-Lopez P, Brito R, Soto R (2011) Dynamical approach to the casimir effect. Phys Rev E 83: 031102–031113.
40. Bitbol AF, Fournier JB (2011) Forces exerted by a correlated fluid on embedded inclusions. Phys Rev E 83: 061107–061120.
41. Lambrecht A, Jaekel MT, Reynaud S (1996) Motion induced radiation from a vibrating cavity. Phys Rev Lett 77: 615–618.
42. Davis P (1996) Shaking light from the void. Nature 382: 761–762.
43. Golestanian R, Kardar M (1997) Mechanical response of vacuum. Phys Rev Lett 78: 3421–3425.
44. Golestanian R, Kardar M (1998) Path-integral approach to the dynamic casimir effect with fluctuating boundaries. Phys Rev A 58: 1713–1722.
45. Bialynicki-Birula I, Bialynicka-Birula Z (2008) Dynamical casimir effect in oscillating media. Phys Rev A 78: 042109–042116.
46. Scheel S, Buhrmann SY (2009) Casimir-polder forces on moving atoms. Phys Rev A 80: 042902–042912.
47. Krüger M, Emig T, Kardar M (2011) Nonequilibrium electromagnetic fluctuations: Heat transfer and interactions. Phys Rev Lett 106: 210404–210407.
48. Krüger M, Emig T, Bimonte G, Kardar M (2011) Non-equilibrium casimir forces: Spheres and sphere-plate. EPL 95: 21002–21007.
49. Sheng S, Narayanaswamy A, Chen G (2009) Surface phonon polaritons mediated energy transfer between nanoscale gaps. Nano Lett 9: 2909–2913.
50. Rousseau E, Siria A, Jourdan G, Volz S, Comin F, et al. (2009) Radiative heat transfer at the nanoscale. Nat Photon 3: 514–517.
51. Bray AJ (1994) Theory of phase-ordering kinetics. Adv Phys 43: 357–459.
52. Folk R, Moser G (2006) Critical dynamics: a field-theoretical approach. J Phys A: Math Gen 39: R207–R313.
53. Siggia ED, Halperin BI, Hohenberg PC (1976) Renormalization-group treatment of the critical dynamics of the binary-fluid and gas-liquid transitions. Phys Rev B 13: 2110–2123.
54. Halperin BI, Hohenberg PC, Siggia ED (1976) Renormalization-group treatment of the critical dynamics of superfluid helium, the isotropic antiferromagnet, and the easy-plane ferromagnet. Phys Rev B 13: 1299–1328.
55. Chandler D (1987) Introduction to Modern Statistical Mechanics. New York: Oxford University Press.
56. Gambassi A, Dietrich S (2006) Critical dynamics in thin films. J Stat Phys 123: 929–1005.
57. Lauga E, Powers TR (2009) The hydrodynamics of swimming microorganisms. Rep Prog Phys 72: 096601–096636.
58. Clarke RJ, Cox SM, Williams PM, Jensen OE (2005) The drag on a microcantilever oscillating near a wall. J Fluid Mech 545: 397–426.
59. Chadwick RS, Liao Z (2008) High-frequency oscillations of a sphere in a viscous fluid near a rigid plane. SIAM Rev Soc Ind Appl Math 50: 313–322.
60. Hanke A, Kardar M (2001) Modified critical correlations close to modulated and rough surfaces. Phys Rev Lett 86: 4596–4599.
61. Hanke A, Kardar M (2002) Correlation functions near modulated and rough surfaces. Phys Rev E 65: 046121–046134.